

“Single-” and “multi-core” FePt nanoparticles: from controlled synthesis via zwitterionic and silica bio-functionalization to MRI applications

Nina Kostevšek · Sašo Šturm · Igor Serša · Ana Sepe ·
Maarten Bloemen · Thierry Verbiest · Spomenka Kobe ·
Kristina Žužek Rožman

Received: 27 August 2015 / Accepted: 21 November 2015 / Published online: 30 November 2015
© Springer Science+Business Media Dordrecht 2015

Abstract The value of the magnetization has a strong influence on the performance of nanoparticles that act as the contrast agent material for MRI. In this article, we describe processing routes for the synthesis of FePt nanoparticles of different sizes, which, as a result, exhibit different magnetization values. “Single-core” FePt nanoparticles of different sizes (3–15 nm) were prepared via one-step or two-step synthesis, with the latter exhibiting twice the magnetization ($m_{(1.5T)} = 14.5$ emu/g) of the nanoparticles formed via the one-step synthesis ($m_{(1.5T)} < 8$ emu/g).

Furthermore, we propose the synthesis of “multi-core” FePt nanoparticles by changing the ratio between the two surfactants (oleylamine and oleic acid). The step from smaller “single-core” FePt nanoparticles towards the larger, “multi-core” FePt nanoparticles (>20 nm) leads to an increase in the magnetization $m_{(1.5T)}$ from 8 to 19.5 emu/g, without exceeding the superparamagnetic limit. Stable water suspensions were prepared using two different approaches: (a) functionalization with a biocompatible, zwitterionic, catechol ligand, which was used on the FePt nanoparticles for the first time, and (b) coating with SiO₂ shells of various thicknesses. These FePt-based nanostructures, the catechol- and SiO₂-coated “single-core” and “multi-core” FePt nanoparticles, were investigated in terms of the relaxation rates. The higher r_2 values obtained for the “multi-core” FePt nanoparticles compared to that for the “single-core” ones indicate the superiority of the “multi-core” FePt nanoparticles as T_2 contrast agents. Furthermore, it was shown that the SiO₂ coating reduces the r_1 and r_2 relaxation values for both the “single-core” and “multi-core” FePt nanoparticles. The high r_2/r_1 ratios obtained in our study put FePt nanoparticles near the top of the list of candidate materials for use in MRI.

Electronic supplementary material The online version of this article (doi:10.1007/s11051-015-3278-9) contains supplementary material, which is available to authorized users.

N. Kostevšek (✉) · S. Šturm · S. Kobe ·
K. Žužek Rožman
Department for Nanostructured Materials, Jožef Stefan
Institute, Jamova 39, Ljubljana, Slovenia
e-mail: nina.kostevsek@ijs.si

N. Kostevšek
Jožef Stefan International Postgraduate School, Jamova
39, Ljubljana, Slovenia

I. Serša · A. Sepe
Department for Condensed Matter Physics, Jožef Stefan
Institute, Jamova 39, Ljubljana, Slovenia

M. Bloemen · T. Verbiest
Department of Chemistry, KU Leuven, Celestijnenlaan
200D, Heverlee, Belgium

Keywords FePt nanoparticle · Single-core · Multi-core · Zwitterionic dopamine ligand · Relaxivity · Magnetic nanoparticles

Introduction

The research and development of magnetic nanoparticles is now at the stage of a top-down design, where specific application demands govern the material choice and the synthesis methods applied. However, an awareness of the potentials and limitations of the material itself, as well as the capabilities of the synthesis methods, have to be considered. Of course, the choice of material is primarily determined by the intrinsic properties. The magnetic properties of the *fcc* FePt system include a high Curie temperature and a high bulk saturation magnetization [(M_s) , i.e. about 1140 emu/cm^3 — 75 emu/g ($\rho = 14 \text{ kg/m}^3$)] (Wu et al. 2004; Maenosono and Saita 2006; Chen and Andre 2012), which along with its good chemical stability (Sun 2000; Maenosono and Saita 2006) promise the possibility of diverse implementations in biomedicine, e.g. separation, immunoassays, gene transfection, cell targeting, drug delivery, hyperthermia and magnetic particle imaging (Thanh 2012). Magnetic resonance imaging (MRI) has been recognized as one of the most important imaging techniques because of its high spatial resolution, strong soft-tissue contrast and the absence of radiation risk (Slichter 1990; Shin et al. 2015). Despite this, the method has limitations when it comes to detecting small biological targets, which is crucial in the early stages of cancer, for example. To tackle this lack of sensitivity, magnetic nanoparticles are employed as MRI contrast enhancement agents. These MRI contrast agents are classified into T_2 - or T_1 -type contrast agents, depending on their relaxivity coefficients (r_2 or r_1 , $\text{mM}^{-1} \text{ s}^{-1}$), which are the terms that define the ability to accelerate the relaxation rates (R_2 or R_1 , s^{-1}) (Shin et al. 2015). The r_2/r_1 ratio is an important parameter to estimate whether a given contrast agent can serve as a T_1 or T_2 contrast agent. T_1 MRI contrast agents need to have a high r_1 and a low r_2/r_1 ratio, e.g. paramagnetic chelates usually have r_2/r_1 ratios of 1–2. In contrast, to be an effective T_2 MRI contrast agent, a high r_2 value is a prerequisite, with the r_2/r_1 ratio equal to 10 or even more (Caravan et al. 1999). Depending on the magnetic properties and surface effects the magnetic nanoparticles can serve as effective T_2 or T_1 MRI contrast agents (Huang et al. 2014).

After considering the use of magnetic nanoparticles in MRI, we mainly focus on the transverse spin

relaxation T_2 . The relationship between the magnetization and the T_2 relaxation rate R_2 is described as follows:

$$R_2 = \frac{1}{T_2} = \frac{256\pi^2\gamma^2}{405} m_s^2 V \frac{r^2}{D(1 + \frac{L}{r})}, \quad (1)$$

where γ is the gyromagnetic ratio of the protons, m_s is the saturation magnetization of the nanoparticle, V is the nanoparticle's volume fraction, r is the radius of the magnetic nanoparticle, D is the diffusion coefficient of the water molecules and L is the thickness of the surface coating (Tong et al. 2010). The equation states that the shortening of T_2 is directly proportional to the square of the saturation magnetization, which suggests that systems exhibiting large saturation magnetization, like FePt, would be of interest. A bulk saturation magnetization (M_s) is an intrinsic magnetic property; however, by reducing the size of the material to the nanoscale, the surface effects on the magnetization (m_s) become significant or even decisive (Shin et al. 2015). The size of the magnetic nanoparticles used for MRI is therefore very important, since it influences the m_s and, consequently, the R_2 . Theoretical studies indicate that there are three different nanoparticle size regimes: (i) the motional average regime (MAR), (ii) the static dephasing regime (SDR) and (iii) the echo-limiting regime (ELR). R_2 increases in the MAR with the nanoparticle size increment and reaches a plateau (SDR). With any further size increment, the R_2 decreases (ELR). Accordingly, the highest R_2 is achieved for the nanoparticles in the SDR, but the size of the nanoparticles used for MRI usually falls into the MAR in order to limit their uncontrolled aggregation, induced by strong ferromagnetic dipolar interactions (Shin et al. 2015). Even though the M_s of a FePt alloy is high, it is very difficult to achieve this value when the material is in a nanoparticle form. The saturation magnetization of the nanoparticles is known to be proportional to the nanoparticles' size, according to the relation:

$$m_s = M_s [(r - d)/r]^3, \quad (2)$$

where M_s is the saturation magnetization of the bulk, r is the radius of the nanoparticle and d is the thickness of the disordered surface spin layer (Wu et al. 2004; Tanaka et al. 2008; Na et al. 2009). The disordered layer thickness is usually in the range below 1 nm to several nm. For 9-nm FePt nanoparticles, it is

estimated to be 1.5–1.8 nm, depending on the surface ligand (Tanaka et al. 2008). By increasing the size of the FePt nanoparticles, the m_s value can be increased, but while remembering to keep the nanoparticles in the superparamagnetic state (17 ± 2 nm for fcc FePt nanoparticles (Sun 2000; Lee et al. 2006a; Nandwana et al. 2007; Zeynali et al. 2012). An additional factor that reduces the M_s is the application of surface functionalization groups on nanoparticles (surfactants), either for the nanoparticle suspension stability and/or for their biocompatibility (Tanaka et al. 2008). It was reported (Wu et al. 2004) that 3-nm-sized FePt nanoparticles exhibit a dramatic increase in the value of m_s from 210 to 850 emu/cm³ when annealed at 400 °C, due to the removal of the surfactant layer, which is magnetically “dead”; however, this causes agglomeration of the nanoparticles, which is not desirable in biomedical applications.

One of the options for improving the nanoparticles' effect on the T_2 relaxation times is to produce controlled clusters of magnetic nanoparticles with an increased m_s to fit the SDR regime. The enhancements of the longitudinal and transverse relaxation rates of the protons in the water are quantified by the relaxivities r_1 and r_2 , respectively. Success in increasing the r_2 was achieved for iron oxide nanoparticles (7.4 nm) combined into clusters (163 nm) in block polymer micelles (Balasubramaniam et al. 2014), where the increase in the loading of iron oxide nanoparticles in the micelles from 12 to 42 % causes an increase in the r_2 from 90 to of 229 mM⁻¹ s⁻¹, which surpasses that of commercial Feridex® (41 mM⁻¹ s⁻¹ at 1.5 T, 37 °C). Alternatively, silica can be used to synthesize the nanoclusters, and improvements in r_2 were achieved for Fe-oxide nanoparticles (Lee et al. 2006b).

In the FePt system, controlled aggregates, i.e. “multi-core” nanoparticles, can be synthesized in situ without any templates. The influence of the surfactant concentration (oleic acid, OA and oleylamine, OLA) on the formation of Fe-oleic acid and Pt-oleylamine complexes was thoroughly described (Saita and Maenosono 2005). It was showed (Green et al. 2014) that “multi-core” FePt nanoparticles can be prepared by changing the amount and the ratio of the used surfactants (oleic acid/oleylamine). In our investigation, a modification of the procedure described by Green et al. (2014) was used.

When talking about the implementation of biomedical FePt nanoparticles, the positive effects on human

health have to be balanced with the possible toxicity (Kim et al. 2005). Up to now, only a limited number of studies have been performed on FePt nanoparticles (Kim et al. 2005; Chou et al. 2010; Yang et al. 2010), where no significant cytotoxic effect was shown; however, the use of biocompatible coatings, such as silica (Lu et al. 2010), provides the necessary biocompatibility and positively influences the nanoparticle size that was found to be the most appropriate between 20 and 100 nm. Such nanoparticles are believed to be easily internalized by cells, in comparison to smaller or larger particles (Elsabagy and Wooley 2012). The SiO₂ surface is, due to the presence of –OH groups, negatively charged at pH values higher than 2 (Stanford et al. 2008), which ensures the colloidal stability but limits the cell internalization. Therefore, in order to promote the cell internalization efficiency and the binding capability for biomedical molecules, 3-aminopropyl triethoxysilane (APTES) is commonly used to introduce positively charged amino groups on the silica surface (Verma and Stellacci 2010; Barisik et al. 2014). In order to evaluate the T_2 -shortening effect in MRI for as-synthesized magnetic nanoparticles, water suspensions are a prerequisite, which is sometimes problematic since the syntheses of FePt nanoparticles are performed in organic solvents. Only a few attempts were reported for water suspensions of FePt nanoparticles using tetramethylammonium hydroxide (Maenosono et al. 2008), cysteamine (Chen et al. 2010b) or mercaptoalkanoic acids (Bagaria et al. 2006). In our study, the functionalization of the FePt nanoparticles was performed with a hydrophilic and biocompatible, zwitterionic, dopamine sulfonate (ZDS) ligand, since it has been demonstrated (Xu et al. 2004) that it can serve as an attractive ligand to render Fe-oxide nanoparticles hydrophilic, due to the strong interaction between the vicinal diol groups and the iron oxide surface, as well as the hydrophilicity of the amide and carbonyl groups. This ligand was found to be suitable for Fe-oxide nanoparticles (Wei et al. 2012), but no attempts to functionalize the FePt nanoparticles with it were reported yet.

Based on the state of the art for FePt nanoparticles used in biomedical applications, our contribution represents a synthesis roadmap: starting from the “single-core” FePt nanoparticle synthesis and leading to “multi-core” nanoparticle synthesis. The ratio of the two surfactants, i.e. oleylamine/oleic acid, was

used to modify the shape of the FePt nanoparticle, while their concentration dictates the size of the nanoparticles. Both parameters have a strong effect on the magnetic properties of the synthesized nanoparticles, thereby increasing their m_s and, consequently, the r_2 . Stable water suspensions of “single-core” and “multi-core” FePt nanoparticles were obtained by using two different approaches: (a) for the first time, a functionalization with biocompatible, zwitterionic, catechol ligands was performed or (b) SiO₂ coating of both species “single-core” and “multi-core” resulted in biocompatible FePt nanoparticle suspensions. Such functionalized FePt nanoparticle suspensions, with an r_2 suitable for MRI, represent a comprehensive system that is appropriate for various biomedical applications.

Experimental

For the synthesis of the FePt nanoparticles, a hemispherical heating mantle (model WiseTherm WHM 12112 from Witeg Labortechnik GmbH) connected to a temperature controller (J-KEM, model 310) with a J-type Teflon thermocouple was used. The samples were characterized using a (scanning) transmission electron microscope (TEM Jeol JEM-2010F) equipped with energy-dispersive X-ray spectroscopy (EDXS). The powder X-ray diffraction was measured using a Siemens D5000 diffractometer with a Cu-K α source ($\lambda = 1.5406 \text{ \AA}$), and the magnetic measurements were performed with a vibrating sample magnetometer (VSM) MicroSense model FCM 10 operated at room temperature. In order to determine an accurate amount of FePt in the sample, thermogravimetric analyses (TG analyser NETZSCH STA 449 C/6/G Jupiter) were performed to determine the amount of organic matter in the sample (30 %). The magnetization values are reported for the mass of FePt in the sample after the subtraction of the organic content. Water suspensions of catechol-functionalized and SiO₂-coated “single-core” and “multi-core” FePt nanoparticles were prepared with different concentrations (0.01–0.08 mM with respect to the Fe content), and the T_1 and T_2 relaxation times were measured. The measurements were made on an NMR/MRI system consisting of a 2.35-T superconducting magnet (Oxford Instruments, Abingdon, UK) and an Apollo NMR spectrometer (TecMag, Houston TX, USA). The T_1

relaxation times were measured using an inversion recovery sequence with 16 different inversion times, ranging from 100 μ s to 10 s, while the T_2 relaxation times were measured using the Carr Purcell Meiboom Gill (CPMG) sequence with multiple spin-echoes. The T_1 and T_2 relaxation times were calculated from the best fits between the measurements and the corresponding model for either T_2 relaxation (exponential dependency of the echo-signal on the echo number) or T_1 relaxation (dependency of the inversion recovery signal on the inversion time). The calculations were performed using the Origin program (OriginLab Corporation, Northampton MA, USA).

The dependencies of the longitudinal ($1/T_1$) and transverse ($1/T_2$) relaxation rates on the FePt nanoparticles' concentration were used to extract the FePt nanoparticles' relaxivities r_1 and r_2 . These are defined as proportionality constants between the contrast agent-induced increase of the corresponding relaxation rate and the MR contrast agent concentration.

$$r_1 = \frac{\left(\frac{1}{T_1}\right)_C - \left(\frac{1}{T_1}\right)_0}{C}, r_2 = \frac{\left(\frac{1}{T_2}\right)_C - \left(\frac{1}{T_2}\right)_0}{C}. \quad (3)$$

Here, C denotes the contrast agent concentration, while the indexes C and 0 denote the relaxation rates at the contrast agent concentration C and at zero concentration, respectively. For each type of FePt nanoparticles, the relaxivities r_1 and r_2 were calculated from the best fit between the model given in Eq. (3) and the relaxation-time measurements.

Results and discussion

“Single-core” FePt nanoparticles synthesis based on varying the amount of surfactants

“Single-core” FePt nanoparticles (Table 1, S1–S8) were synthesized using a modification of the polyol method, reported by Sun's group, in an argon atmosphere (Sun 2000). The TEM images in Fig. 1 represent the FePt nanoparticles prepared by the addition of different volumes of both surfactants, 0.5 mL (S2) and 4 mL (S7), where the sizes of the FePt nanoparticles were found to be 3 nm (Fig. 1a) and 6 nm (Fig. 1b), respectively. For the largest added volume (6 mL, S8), the size is increased to 7.5 nm (Fig. 1c); however, the nanoparticles start to

Table 1 Sample list of FePt nanoparticles, including the amounts of OLA and OA used and the resulting OLA/OA ratio for FePt samples 1–17; Fe(acac)₃ (1 mmol, 70 mg) and Pt(acac)₂ (0.5 mmol, 40 mg) were used in dibenzyl ether (20 mL) and 1,2-hexadecanediol (2.3 mmol, 0.012 g)

Sample	OLA/mL	OA/mL	Ratio OLA:OA	Nanoparticles form
1	0.15	0.15	1:1	“Single-core”
2	0.5	0.5	1:1	“Single-core”
3	0.6	0.6	1:1	“Single-core”
4	1.5	1.5	1:1	“Single-core”
5	2.5	2.5	1:1	“Single-core”
6	3	3	1:1	“Single-core”
7	4	4	1:1	“Single-core”
8	6	6	1:1	“Single-core”
9	6	0	6:0	“Multi-core”
10	6	0.5	6:0.5	“Multi-core”
11	6	1	6:1	“Multi-core”
12	6	2	6:2	“Multi-core”
13	6	3	6:3	“Multi-core”
14	6	4.5	6:4.5	“Multi-core”
15	0	6	0:6	“Single-core”
16	4	1.3	6:3	“Multi-core”
17	2	0.66	6:3	“Multi-core”

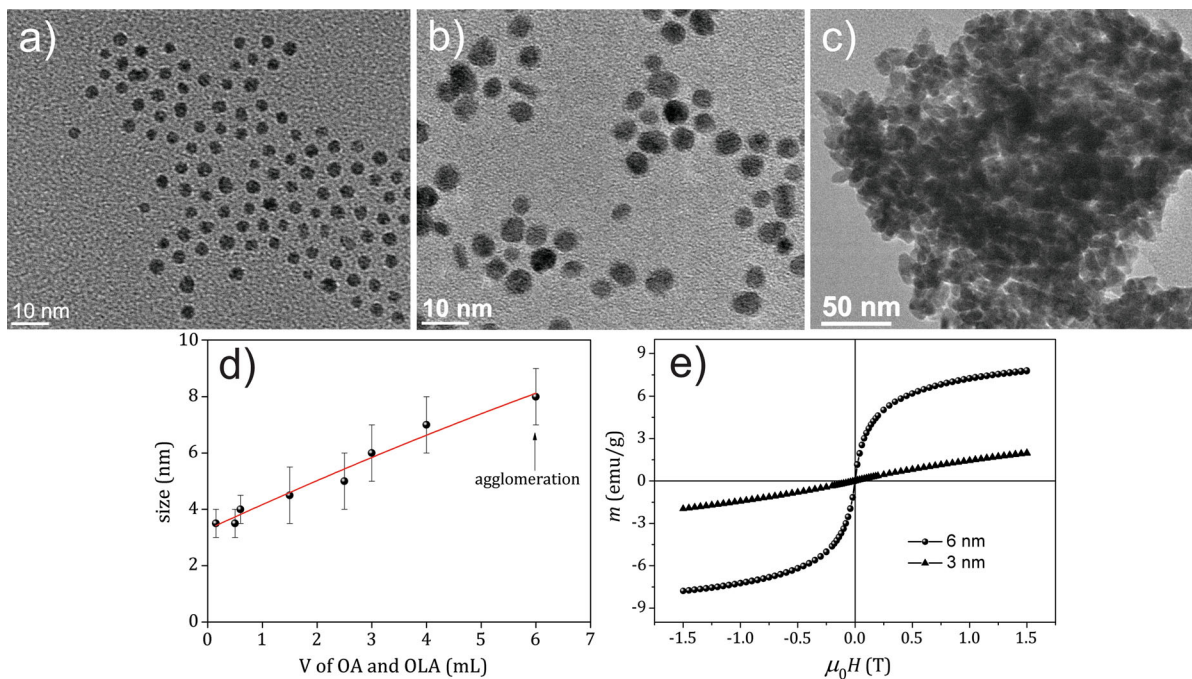


Fig. 1 TEM images for **a** 3-nm (S2), **b** 6-nm (S7) and **c** agglomerated (S8) “single-core” FePt nanoparticles. **d** Graph indicating the size of “single-core” FePt nanoparticles

for different amounts of added surfactants and **e** comparison of the magnetic properties for 3- and 6-nm “single-core” FePt nanoparticles measured at 300 K

agglomerate, since at higher surfactant concentrations, the free surfactant molecules can cause flocculation of the already surfactant-stabilized nanoparticles, which

is in accordance with the literature observations (Nandwana et al. 2007) and with the proposed nucleation-and-growth mechanism (Shevchenko

et al. 2003). A graph indicating the linear dependence of the particle size on the volume of the added surfactants is shown in Fig. 1d. The hysteresis loops measured at 300 K for the furthest-apart samples in terms of their size (3 and 6 nm) are shown in Fig. 1e. Both samples exhibit superparamagnetic behaviour, with the magnetizations $m_{(1.5T)}$ 2 and 8 emu/g, respectively. Our measured values for the magnetization are comparable to the values reported in the literature for similarly sized FePt nanoparticles (Kim et al. 2005; Nandwana et al. 2007). However, the still relatively low m_s values, in comparison with the bulk FePt M_s value, are most probably due to the particle size reduction according to Eq. (2) or due to the functionalization of the nanoparticles with the surfactants, which causes a magnetically “dead” surface layer due to the oxygen bonds of the surfactant polar end group (oleic acid/oleylamine) with Fe (Wu et al. 2004). It was reported that by removing/decomposing the surfactant layer, the M_s of the FePt nanoparticles can be fully recovered (Wu et al. 2004), but this causes agglomeration of the nanoparticles, which is not desirable for biomedical applications.

“Single-core” FePt nanoparticles synthesis based on seed-mediated growth

In order to grow larger nanoparticles with a higher m_s , a two-step synthesis, i.e. seed-mediated growth (Zeynali et al. 2012), was performed. For the first step in the synthesis, the experimental conditions for the formation of well-dispersed, 6-nm-sized FePt nanoparticles were used (S7, Fig. 1b). In the second step, half of the initial volume of the metal salts was added, and the same heating regime was used as in the first step. From

the TEM micrograph (Fig. 2a) of the nanoparticles formed in the second step, it is clear that the nanoparticles grew to sizes up to 15 nm after the second step with very few smaller seeds remaining; however, the nanoparticles developed an irregular shape. The magnetization value after the second step was almost twice as large (14.5 emu/g) as after the first step (8 emu/g). The hysteresis loop presented in Fig. 2b shows that the larger particles maintained their superparamagnetic behaviour; however, the size of the formed nanoparticles is already at the superparamagnetic *fcc* FePt size limit (17 nm), which could restrict their use in biomedical applications.

“Multi-core” FePt nanoparticles synthesis

In order to improve the magnetic properties further, keeping in mind the superparamagnetic size limit (D_s), we focused on the growth of “multi-core” FePt nanoparticles by using the modified procedure described in the literature (Green et al. 2014). Such FePt “multi-core” nanoparticles were proven to exhibit larger m_s values than their “single-core” counterparts. In order to systematically study the formation of “multi-core” FePt nanoparticles, the ratio between the OLA and the OA was varied from 0.08 to 0.75. The volume of OLA was constant (6 mL), while the volume of OA was varied: 0, 0.5, 1, 2, 3 and 4.5 mL (S9–S14). When the amount of added OA was larger than the amount of OLA ($OA > OLA$), “single-core” FePt nanoparticles were always obtained (data not shown). TEM images of the prepared samples with different OLA-to-OA ratios are shown in Fig. 3. It is evident that a small amount of OLA is needed to stabilize the nanoparticles and to

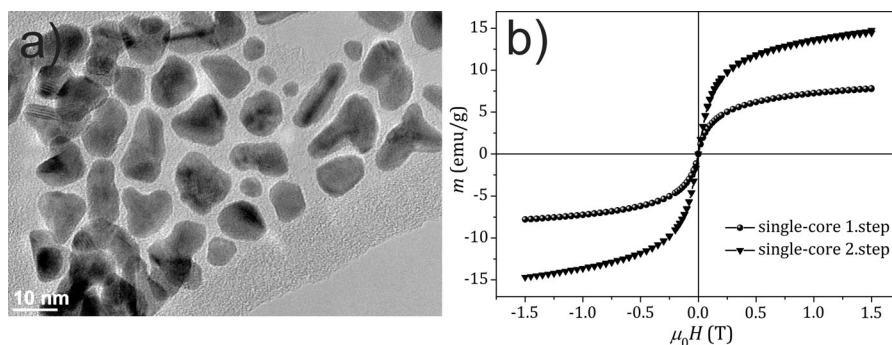


Fig. 2 **a** TEM image of nanoparticles obtained after step 2 of the seed-mediated growth with **b** the corresponding magnetic measurements for the nanoparticles after steps 1 and 2 at 300 K

prevent agglomeration, which occurs when only OA is used as the surfactant (S15, Fig. 3; OLA:OA ratio = 0:6). It is clear from the TEM images in Fig. 3 that when the amount of added OLA is larger than the amount of OA (OLA > OA), “multi-core” FePt nanoparticles can be obtained. Moreover, a higher OLA:OA ratio leads to a slight decrease in the size of the “multi-core” nanoparticles, with a smaller size (approx. 10 nm) being obtained when only OLA was used (Fig. 3; OLA:OA ratio = 6:0). In all of the cases when OLA > OA “multi-core” nanoparticles with slightly elongated “single-core” nanoparticle shapes were formed, the nanoparticle aspect ratio was found to decrease with OA addition. The observed elongated shape of the synthesized nanoparticles has its roots in OLA-induced, one-dimensional growth as observed in the literature (Wang et al. 2007; Chou et al. 2009). The latter group reported that the growth rates for the {111} and {100} planes in the FePt *fcc* crystal structure can be affected by changing the OLA:OA ratio. The amine group of OLA binds more strongly on the {100} planes than on the {111} planes, which causes the formation of slightly elongated structures. On the other hand, OA binds on both planes equally and therefore spherical structures are formed. The sample produced at OLA:OA = 6:2 (S12) showed the most consistent “multi-core” morphology, and it was used in all the

subsequent experiments. Magnetic measurement obtained for the FePt “multi-core” nanoparticles (Fig. 3) indicated superparamagnetic behaviour, with an increased $m_{(1.5T)} = 19.5$ emu/g in comparison with the “single-core” FePt nanoparticles.

Typical morphologies and size distributions of the “single-core” and “multi-core” FePt nanoparticles are shown in Fig. 4. The average size (defined as the average diameter) of the “single-core” (S7) nanoparticles measured on the basis of 30 individual particles was 7 ± 1 nm. In the case of the “multi-core” nanoparticles (S12), the average size was determined by measuring the average diameter of the body, using the dashed line, as indicated in Fig. 4b. The average particle size of the “multi-core” nanoparticles was 20 ± 3 nm.

The selected area electron diffraction (SAED) patterns (superimposed in Fig. 4), which were obtained for the “single-core” and “multi-core” samples, are in accordance with the *fcc* crystal structure of the FePt phase (Dai et al. 2001). No additional phases could be detected, either using TEM/STEM imaging or electron diffraction techniques (e.g. oxide phases, etc.). The elemental analysis obtained using the EDXS was performed on “single-core” (S7) and “multi-core” (S12) samples. Three separately prepared samples for the “single-core” and “multi-core” FePt nanoparticles were examined for their

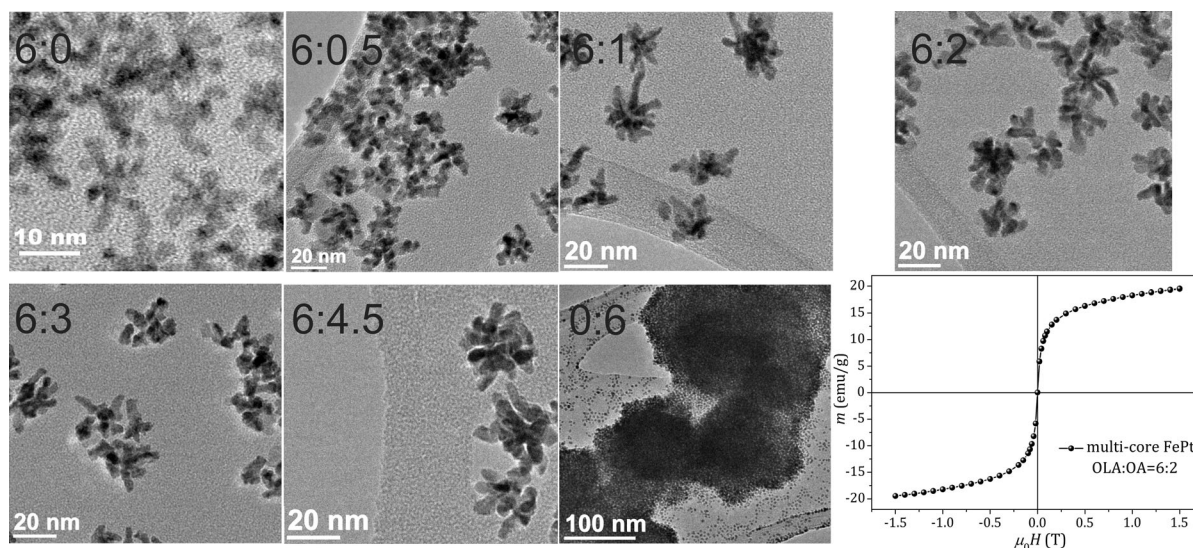
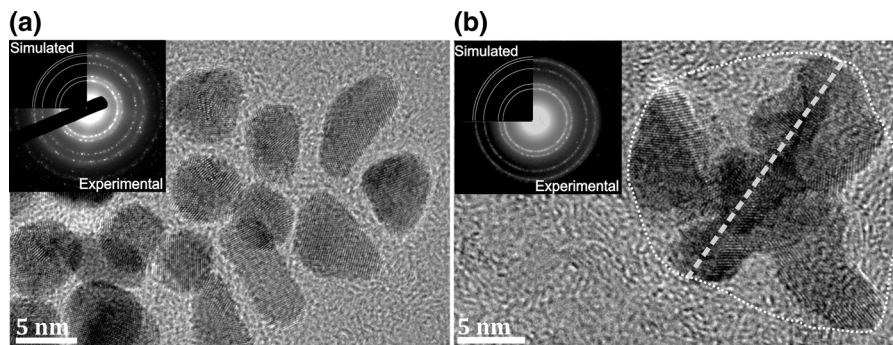


Fig. 3 TEM images of “multi-core” FePt nanoparticles for different OLA:OA ratios with magnetic measurements at 300 K for the sample with OLA:OA ratio = 6:2 (S12)

Fig. 4 HR-TEM images of **a** “single-core” and **b** “multi-core” FePt nanoparticles with corresponding SAED patterns shown as *insets*



elemental composition in order to estimate the reproducibility of the synthesis procedure, and five spectra were recorded for each sample in different areas. All three “single-core” or “multi-core” samples had very similar compositions, with the maximum deviation between them being ± 1 at.%. The elemental composition determined from the obtained EDXS data for the “single-core” or “multi-core” samples was $\text{Fe}_{25\pm 1}\text{Pt}_{75\pm 1}$ and $\text{Fe}_{30\pm 1}\text{Pt}_{70\pm 1}$, respectively. A slightly higher content of Fe in the case of the “multi-core” FePt nanoparticles can be attributed to the lower content of OA during the synthesis. It was suggested that OA is a coordinative ligand for the Fe atoms, and OLA is said to coordinate the Pt intermediates (Saita and Maenosono 2005). Therefore, a smaller amount of OA would result in a fewer coordinated Fe metal intermediates in the reaction mixture and hence nanoparticles with a slightly higher Fe content.

In order to determine the crystallinity of the individual “single-core” and “multi-core” nanoparticles, a series of atomic-resolution high-angle annular dark-field STEM (HAADF-STEM) images were acquired. Representative HAADF-STEM images are shown in Fig. 5. The HAADF-STEM image acquired from the “single-core” nanoparticle in the [112] projection of the FePt *fcc* structure is shown in Fig. 5a, and the enlarged region of the particle edge is shown as an inset. The observed non-periodic variation of high and low intensity between the adjacent atomic columns, which is marked by white and grey arrows (Fig. 5a), is directly related to the non-periodic variations in the atomic-column composition, thus described as a FePt solid solution with a *fcc* structure, which is in accordance with the SAED analysis. The HAADF-STEM images of the “multi-core” nanoparticles (Fig. 5b) show that these aggregates are

typically composed of radially grown, individual nanoparticles. The structural characteristics of these individual particles are the same as described for the case of the “single-core” nanoparticles. The results showed that controlled aggregates, i.e. “multi-core” FePt nanoparticles, can be synthesized in situ without any templates. It was reported (Green et al. 2014) that “multi-core” FePt nanoparticles can be prepared by changing the amount and the ratio of the used surfactants (oleic acid/oleylamine). However, we have selected a different Fe precursor in order to have similar metal salts ($\text{Pt}(\text{acac})_2$ and $\text{Fe}(\text{acac})_3$), which facilitate the formation of a pure FePt phase (solid solution) that was confirmed by detailed TEM analysis. Moreover, during our research, it was ascertained that the addition of a small amount of a reducing agent is necessary to avoid the oxidation of FePt NPs and the formation of oxide phases. TEM analyses confirmed a pure FePt phase without any oxide phase present. Therefore, in this study, during the synthesis, a reducing agent (1,2-hexadecanediol) was added. In contrast, in the work of Green et al., a thin iron oxide layer is reported, most probably due to the fact that no reducing agent was used.

Functionalization of “single- & multi-core” FePt nanoparticles with zwitterionic dopamine sulfonate

The as-synthesized FePt nanoparticles are hydrophobic due to the use of OLA and OA as the surfactants. In order to transfer them into a water phase, we used the ZDS ligand. The benefits of using the ZDS ligand lie in its chemical character, since it is composed of three active moieties (Wei et al. 2012). The dopamine provides a strong coordination to the nanoparticle

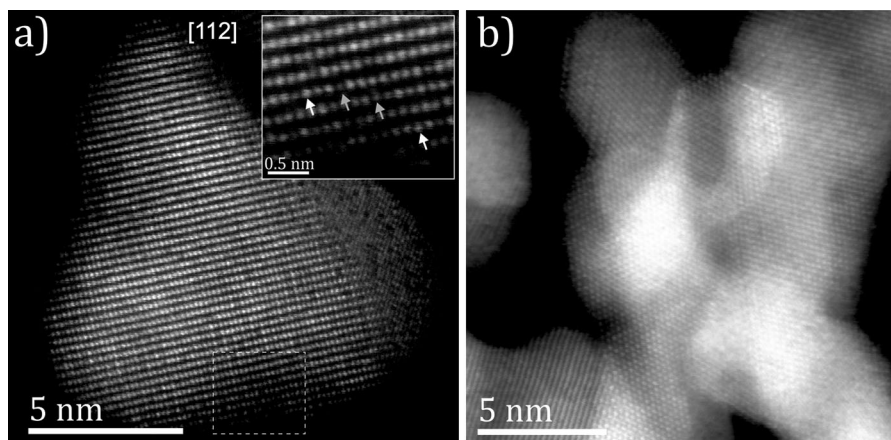


Fig. 5 High-resolution HAADF-STEM images of individual **a** “single-core” and **b** “multi-core” FePt nanoparticles. The *inset* shows the enlarged region of the particle’s edge

surface (Xu et al. 2004), the sulfonate group is responsible for the high water solubility and the combination of a quaternary amine group and a sulfonate group gives the ligand a zwitterionic character, which enables its buffer capacity, i.e. a high pH stability, which decreases the nanoparticles’ non-specific interactions with proteins. The ZDS ligand was prepared according to a modified protocol described in the literature (Wei et al. 2012). Dopamine hydrochloride was used as the starting material, with its chemical formula shown in Fig. 6a. Ammonium hydroxide and 1,3-propanesultone were added to induce the sulfonation of the dopamine and the conversion to a dopamine sulfonate (Fig. 6b). To form the final product (ZDS ligand), dopamine sulfonate was dissolved in DMF with the addition of anhydrous sodium carbonate, and the methylation of the amino group was achieved by the addition of iodomethane (Fig. 6c). The excess of base was added to capture the hydrogen iodide that was released (H^+ from amine, I^- from iodomethane) and to keep the system basic, making sure that the amine and the sulphonic acid are not protonated. The protonation of the amine would hinder the nucleophilic attack on the iodomethane. The second methylation is less favourable because of steric hindrance; however, the higher temperature, the already deprotonated sulphonate (hence a more stable end product) and the removal of hydrogen iodide pull the equilibrium to the side of the products. Strong coordination bonds between the $-OH$ groups of the ZDS ligand and the Fe atoms on the

surface of the nanoparticle were already proved in the case of SPIONs (Wei et al. 2012). According to reports in the literature (Hirani et al. 2007), that catechol-Pt complexes were formed by the coordination of Pt onto OH groups of catechol, we can assume that the catechol ligand is also coordinated to Pt atoms, similar to Fe. In Fig. 6d, it is clear that the suspension of oleic acid/oleylamine stabilized the FePt nanoparticles in the hexane phase before the ligand exchange with the nanoparticles-free water phase below. After the ligand-exchange reaction, the ZDS-functionalized FePt nanoparticles are successfully transferred into the water phase and a nanoparticles-free hexane phase is visible above (Fig. 6e). Such ZDS ligand functionalized FePt “single-core” and “multi-core” nanoparticles were subsequently checked for their MRI performance and referred to as “sample S” and “sample M”, respectively.

Functionalization of “single- & multi-core” FePt nanoparticles with SiO_2 and APTES

In order to reduce the possible cytotoxic effects of the FePt nanosystem and to make the FePt nanoparticles’ cell intervention appropriate (Lu et al. 2010), the as-synthesized “single-core” and “multi-core” FePt nanoparticles were covered with SiO_2 shells using the water-in-oil microemulsion method (Lee et al. 2006a). TEM images of the SiO_2 -coated “single-core” and “multi-core” FePt nanoparticles after 24 h of synthesis are shown in Fig. 7b, c, respectively. All the

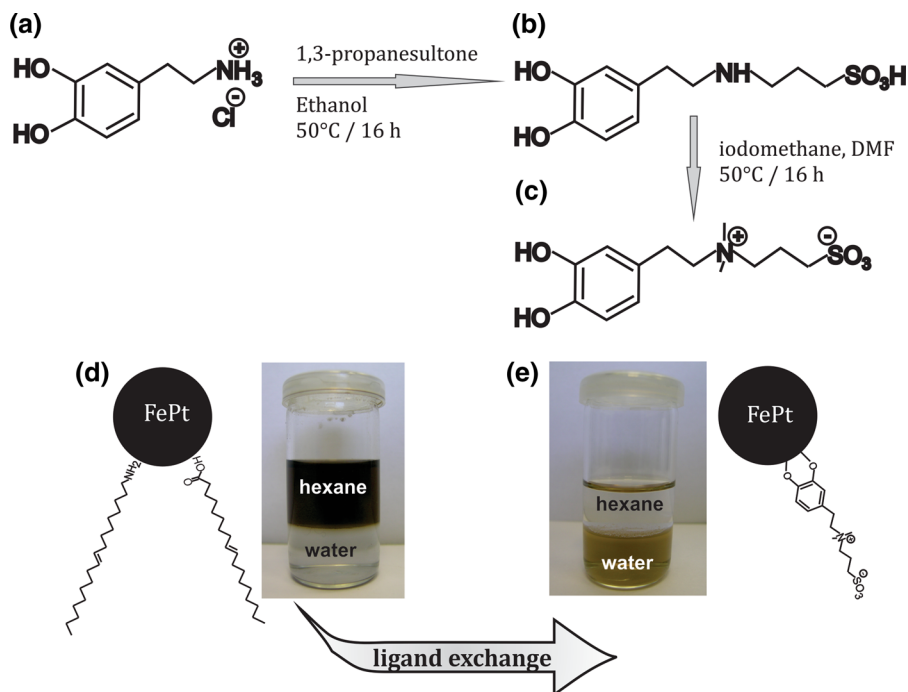


Fig. 6 a–c Synthesis route of the ZDS ligand, **d** oleic acid/oleylamine stabilized FePt nanoparticles in hexane phase before the ligand exchange and **e** ZDS-functionalized FePt nanoparticles in the water phase after the ligand-exchange reaction

FePt nanoparticles are equally covered and no free FePt nanoparticles were found, indicating the successful SiO₂ coating of all the magnetic cores. In

Fig. 7a, the thicknesses of the SiO₂ shells measured after different reaction times (6, 12, 18 and 24 h) are presented for “single-core” or “multi-core” FePt

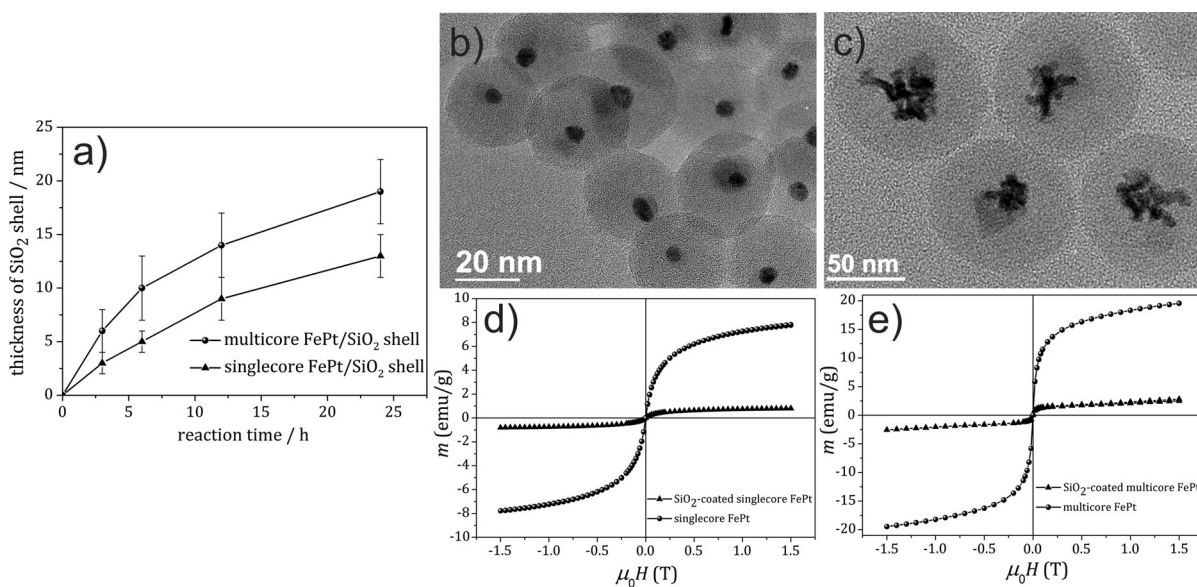


Fig. 7 a Growth of SiO₂ shell with the reaction time, SiO₂-coated **b** “single-core” and **c** “multi-core” FePt nanoparticles with **d**, **e** the corresponding magnetic measurements at 300 K

nanoparticles. The growth of the SiO₂ shell is fast during the first 10 h of the reaction: the increases in the thicknesses of the SiO₂ shells are ~1 nm/h and ~2 nm/h for “single-core” and “multi-core” FePt nanoparticles, respectively. Longer reaction times resulted in linear growth with an approximate growth rate of ~0.5 and ~0.8 nm/h for “single-core” and “multi-core” FePt nanoparticles, respectively. After 24 h of synthesis, the thicknesses of the SiO₂ shells on the “single-core” and “multi-core” FePt nanoparticles were ~12 and ~18 nm, respectively. The same mass of FePt nanoparticles was used in both cases (20 mg). However, the same mass of FePt nanoparticles equals a smaller number of nanoparticles in the case of the “multi-core” sample. Therefore, for each “multi-core” nanoparticle, a larger quantity of reagents is present and consequently a thicker shell is formed. A comparison of the magnetic properties at 300 K before and after the SiO₂ coating for 24 h of “single-core” and “multi-core” FePt nanoparticles is shown in Fig. 7d, e. The $m_{(1.5T)}$ of the SiO₂-coated FePt nanoparticles is equal to ~1 and ~2 emu/g, for “single-core” and “multi-core” nanoparticles, respectively, which is approximately 9 times lower than for the initial FePt nanoparticles in both cases (“single-core” with $m_{(1.5T)} = 8$ emu/g, and “multi-core” with $m_{(1.5T)} = 19.5$ emu/g). The nanoparticles’ surface chemistry can significantly modify their magnetic properties. A FTIR study of FePt nanoparticles stabilized with OLA and OA and further coated with a SiO₂ shell (Aslam et al. 2005) showed that the SiO₂ coating does not deteriorate the amine and carboxylate layer on the FePt surface. From this, it can be concluded that the OLA and OA layer remains on the FePt surface even after the SiO₂ coating and no direct FePt–SiO₂ bonds are formed, which might have an influence on the magnetic properties of the nanoparticles. Because the SiO₂-coating does not induce any change in the chemical bond on the surface of the FePt nanoparticle, the lower magnetization obtained for the SiO₂-coated FePt nanoparticles is merely due to the dilution of the sample with the non-magnetic SiO₂ phase (the magnetization is based on the mass of the whole sample). However, as pointed out in the introduction, the targeted “composite” nanoparticle size was between 20 and 100 nm (Elsabahy and Wooley 2012), which means that the magnetization reduction is inevitable in these kinds of “hybrid” systems with a constant trade-off between

good magnetic properties (large m_s) and good biocompatibility.

In order to further assess the FePt–SiO₂ “composite” material in terms of biomedical applications, its potential in cell internalization was increased by introducing the positively charged aminopropylsilane groups on the SiO₂ surface of the SiO₂-coated “single-core” and “multi-core” FePt nanoparticles. The zeta-potential measured on the APTES-functionalized FePt/SiO₂ nanoparticles was converted from negative for the as-synthesized samples to highly positive after APTES functionalization, with the maximum value being in the pH range 4–7 (Kostevšek et al. 2015). APTES-functionalized SiO₂-coated “single-core” and “multi-core” FePt nanoparticles were used in the MRI measurements and are subsequently referred to as “sample S–SiO₂” and “sample M–SiO₂”, respectively.

ZDS-functionalized and SiO₂-coated “single-core” and “multi-core” FePt as MRI contrast agents

The effectiveness of the ZDS-functionalized and silica-coated “single-core” and “multi-core” FePt nanoparticles as MRI contrast agents was investigated by measuring the dependence of the longitudinal (T_1) and transverse (T_2) relaxation times on the FePt nanoparticles’ concentration. Water suspensions of ZDS-functionalized “single-core” and “multi-core” FePt nanoparticles (sample S and sample M, respectively) and SiO₂-coated “single-core” and “multi-core” FePt nanoparticles (sample S–SiO₂ and sample M–SiO₂, respectively) were prepared with different concentrations (0.01–0.08 mM) with respect to the Fe content. The values of the longitudinal relaxation rate increase $1/T_1 - 1/T_1(0)$ for all four samples (S, M, S–SiO₂ and M–SiO₂) can be found in Fig. 8a, and the corresponding calculated longitudinal relaxivities (r_1) are listed in Table 2. From the r_1 values, it can be concluded that the “single-core” FePt nanoparticles (sample S, $r_1 = 3.6 \pm 0.2$ mM⁻¹ s⁻¹) have a weaker effect on the shortening of the T_1 time than the “multi-core” FePt nanoparticles (sample M, $r_1 = 6.7 \pm 0.7$ mM⁻¹ s⁻¹). The difference is found to be approximately 1.8 times in favour of sample M. In general, there are two relaxations of water protons nearby magnetic nanoparticles, depending on whether the water protons merely diffuse through the magnetic nanoparticles (“outer sphere”) or temporarily bind to

Fig. 8 Graph indicating **a** inverse longitudinal $1/T_1 - 1/T_1(0)$ and **b** inverse transverse $1/T_2 - 1/T_2(0)$ relaxation rate increase for “single-core” (S), “multi-core” (M), SiO₂-coated “single-core” (S-SiO₂) and SiO₂-coated “multi-core” FePt nanoparticles (M-SiO₂)

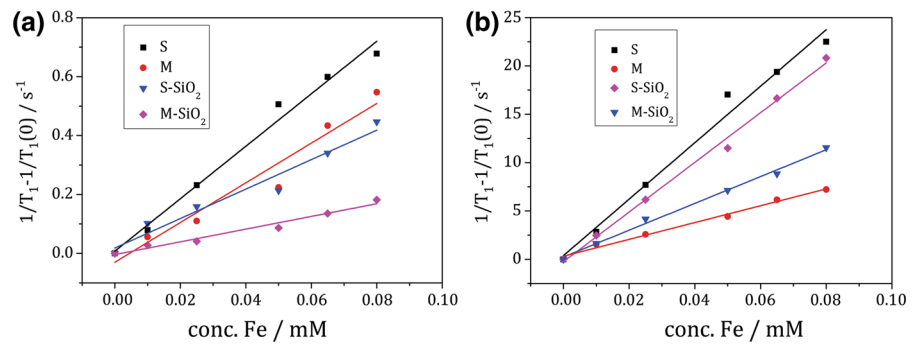


Table 2 Calculated longitudinal (r_1) and transverse (r_2) relaxivities for “single-core” (S), “multi-core” (M), SiO₂-coated “single-core” (S-SiO₂) and SiO₂-coated “multi-core” (M-SiO₂) FePt nanoparticles with corresponding r_2/r_1 ratios

Sample	r_1 (mM ⁻¹ s ⁻¹)	r_2 (mM ⁻¹ s ⁻¹)	r_2/r_1
S	3.6 ± 0.2	52 ± 5	14.4
S-SiO ₂	1.2 ± 0.1	16 ± 2	13.3
M	6.7 ± 0.7	87 ± 4	12.9
M-SiO ₂	2.1 ± 0.2	53 ± 3	25.2

them (“inner sphere”) (Huang et al. 2014). T_1 relaxation enhancement is mainly related to the inner sphere regime that water protons chemically exchange with the surface centres directly. For the smaller magnetic nanoparticles, the spin-canting effect becomes stronger due to the higher fraction of surface metal ions relative to the core ones. This might lead to a decrease in the number of the effective metal centres on the surface and, consequently, less effective coordinating of the water molecules and chemical exchanging of the protons (Huang et al. 2014); therefore, the resulting r_1 value for the smaller “single-core” nanoparticles is lower than in the case of the larger “multi-core” ones. Furthermore, SiO₂-coating reduces the r_1 values for both the “single-core” (sample S-SiO₂, $r_1 = 1.2 \pm 0.1$ mM⁻¹ s⁻¹) and “multi-core” FePt nanoparticles (sample M-SiO₂, $r_1 = 2.1 \pm 0.2$ mM⁻¹ s⁻¹) by approximately 3 times with respect to the uncoated ones.

The values of the transversal relaxation rate increase $1/T_2 - 1/T_2(0)$ for all four samples (S, M, S-SiO₂ and M-SiO₂) can be found in Fig. 8b, and the corresponding calculated transversal relaxivities (r_2) are listed in Table 2. From the relaxivity values r_2 , it is clear that

the “single-core” FePt nanoparticles (sample S, $r_2 = 52 \pm 5$ mM⁻¹ s⁻¹) have a weaker effect on the shortening of the T_2 time than the “multi-core” FePt nanoparticles (sample M, $r_2 = 87 \pm 4$ mM⁻¹ s⁻¹). As was clear from a comparison of the r_1 values, the r_2 values are also approximately 1.7 times higher in the case of sample M. This is in accordance with Eq. (1), where it is clear that R_2 is directly proportional, among other parameters, to $(m_s)^2$, meaning that nanoparticles with higher m_s exhibit higher R_2 and r_2 . Therefore, due to the higher magnetization, “multi-core” nanoparticles (sample M) possess higher r_2 values than the “single-core” ones (sample S). The SiO₂-coating results in a 2- and 3-fold reduction in the r_2 values (sample S-SiO₂, $r_2 = 16 \pm 2$ mM⁻¹ s⁻¹ and sample M-SiO₂, $r_2 = 53 \pm 3$ mM⁻¹ s⁻¹) in comparison with the non-coated samples (S and M). This can be attributed to the fact that the SiO₂ layer increases the distance between the water protons and the magnetic FePt core and, therefore, the effective magnetic relaxations of the water protons around the nanoparticles are reduced, which influences the shortening of the T_2 relaxation times (Shin et al. 2015).

As stated in the introduction, the r_2/r_1 ratio is an important parameter to estimate whether a given contrast agent can serve as a T_1 or T_2 contrast agent. Due to their large magnetization values, magnetic nanoparticles are usually classified as T_2 MRI contrast agents (Shin et al. 2015). A high r_2/r_1 ratio is a prerequisite for an efficient T_2 contrast agent, where the r_2/r_1 ratio should be at least 10 (Caravan et al. 1999). From the r_2/r_1 ratios listed in Table 2, it can be concluded that all four samples possess a high r_2/r_1 ratio and even exceed the required value of 10, which put FePt nanoparticles high on the list of the most promising materials for use in MRI.

Few papers can be found where the relaxivities, r_1 and r_2 , of the “single-core” FePt nanoparticles were measured (Chou et al. 2010; Yang et al. 2010; Taylor et al. 2012; Liang et al. 2015). However, large differences in the experimental conditions (applied magnetic field, surrounding medium, surface functionalization, etc.) make any comparison of the results obtained by different research groups difficult. The applied magnetic field strength is known to influence the T_1 measurements; therefore, the absolute T_1 and r_1 values cannot be compared. However, T_2 relaxation times are less influenced by the applied magnetic field, and therefore, a rough comparison with the literature can be made. Chou et al. (2010) have tested the effect of the nanoparticles’ size on their ability to influence the MRI signal for 3-, 6- and 12-nm FePt nanoparticles coated with cysteamine. It was shown that m_s increased from 1.7 to 12.7 emu/g Fe with the increasing size of the nanoparticles. Consequently, 12-nm FePt nanoparticles represented the most effective negative MRI contrast agent. Taylor et al. (2012) measured for octadecylamine-coated 10-nm-sized FePt nanoparticles in agarose an r_2 value of $62.2 \text{ mM}^{-1} \text{ s}^{-1}$, which is comparable with the values obtained in our study. Liang et al. (2015) studied cysteine-coated 3.8-nm-sized FePt nanoparticles and obtained a low r_2 value in an aqueous solution ($r_2 = 16.9 \text{ mM}^{-1} \text{ s}^{-1}$), which favours the FePt nanoparticles synthesized in our study. Furthermore, Yang et al. (2010) showed in their work that tetraethylene glycol/oleic acid-coated 4-nm-large FePt nanoparticles possess a high r_2 value in an aqueous solution ($r_2 = 122 \text{ mM}^{-1} \text{ s}^{-1}$, $m_s = 25 \text{ emu/g}$). However, their r_2 value is found to be higher than in our case. The reason for this lies most probably, firstly, in the higher m_s and, secondly, in the different nanoparticle coatings, which was not quantitatively evaluated. It is evident from the literature that “single-core” FePt nanoparticles possess high r_2 values, which indicates that this material has a strong potential to become an excellent T_2 MRI contrast agent, as we also confirmed in our study. A step towards increasing the m_s value of “single-core” FePt nanoparticles was proven to work, and significant improvements of m_s were observed, which also reflected positively on the MRI material’s performance. Additionally, we have successfully implemented the use of a dopamine-based ligand to transfer the FePt nanoparticles to a water phase,

while maintaining a high colloidal stability. This means that our study represents a crucial and positive step towards water-based suspensions of biocompatible FePt nanoparticles.

We showed that the “multi-core” FePt nanoparticles synthesized in our study exhibit higher r_2 values in comparison to the “single-core” particles and that the SiO₂ coating reduces both the r_1 and r_2 values. However, the r_2/r_1 ratios are found to exceed the value of 10, which was reported to be ideally suited for quantitatively T_2 -weighed MRI (Caravan et al. 1999). Our r_2 values for FePt nanoparticles are, however, still inferior to “multi-core” iron oxides, mainly due to their higher m_s (Ai et al. 2005; Berret et al. 2006; Chen et al. 2010a; Tanaka et al. 2010). But, despite their good magnetic properties, the Fe-oxide nanoparticles were found to have a limited trans-endothelia passage and tissue penetration, since they suffer from rapid clearance by phagocytic cells (Bulte and Kraitchman 2004; Na et al. 2009), which could be limiting in terms of their biomedical implementations.

We are aware that the functionalized FePt “single-” and “multi-core” nanoparticles developed in our study still need to undergo optimization of the materials’ properties, especially when we talk about their magnetization. Future perspectives would include Fe-rich compositions, since Fe is the element carrying the magnetic moment in the FePt compositions, which would also make the material cheaper. Additionally, the surface layer can be optimized in the future in order to increase the r_2 , but this has to be done thoroughly and carefully and be linked with the nanoparticles’ in vivo MRI performances.

Conclusions

Even though the bulk volume saturation magnetization (M_s) of FePt is higher than that of Fe-oxides, the nanoparticle magnetization (m_s) per unit mass remains inferior. FePt m_s can be drastically increased by using a surfactant-assisted synthesis. The “single-core” FePt nanoparticles’ magnetization, which equaled 8 emu/g, was increased to 19 emu/g for “multi-core” FePt nanoparticles by changing the ratio and volume of the added surfactants (OA and OLA), while keeping the FePt nanoparticles in the superparamagnetic range. In order to obtain magnetic suspensions that are stable in water and biocompatible, “single-core” and

“multi-core” FePt nanoparticles were functionalized with a dopamine-based ligand or coated with SiO₂ shells of various thicknesses. A dopamine-based ligand was used for the first time to transfer the FePt nanoparticles to a water phase, and this represents a crucial step that enables their further biomedical implementation. FePt nanoparticles showed promising MRI characteristics, with significant shortening of the transversal relaxation times, i.e. r_2 relaxivities that were equal to 52 mM⁻¹ s⁻¹ for “single core” FePt and 87 mM⁻¹ s⁻¹ for “multi-core” FePt nanoparticles, while exhibiting r_2/r_1 ratios above 10, which are ideal for MRI (Caravan et al. 1999). The non-magnetic SiO₂ coating “diluted” the magnetic effect of the FePt nanoparticles, resulting in a reduced MRI performance.

Taking all of this into account, some fundamental steps towards FePt nanoparticle bio-implementations have been made in our study, especially in the sense of FePt nanoparticle synthesis and m_s improvements, their bio-functionalization and MRI performance, which will positively affect their subsequent in vitro and in vivo functioning.

Supporting information

Information about the used materials, detailed synthesis procedures for the formation of (a) “single-core” FePt nanoparticles, (b) “single-core” FePt nanoparticles produced via seed-mediated growth, (c) “multi-core” FePt nanoparticles, (d) SiO₂-shell formation, (e) synthesis of ZDS ligand and (f) ligand exchange reaction can be found in the Supporting Information File.

Acknowledgments This work was supported by the Slovenian Research Agency (ARRS), Project J2-6760. This work was financially supported by Grant G.0618.11 N of the Fund for Scientific Research Flanders (FWO-V, www.fwo.be); the Agency for Innovation by Science and Technology in Flanders (IWT, www.iwt.be); and the KU Leuven (GOA, www.kuleuven.be). M. B. is grateful for the support from the IWT.

References

- Ai H, Flask C, Weinberg B et al (2005) Magnetite-loaded polymeric micelles as ultrasensitive magnetic-resonance probes. *Adv Mater* 17:1949–1952. doi:10.1002/adma.200401904
- Aslam M, Fu L, Li S, Dravid VP (2005) Silica encapsulation and magnetic properties of FePt nanoparticles. *J Colloid Interface Sci* 290:444–449. doi:10.1016/j.jcis.2005.04.050
- Bagaria HG, Ada ET, Shamsuzzoha M et al (2006) Understanding mercapto ligand exchange on the surface of FePt nanoparticles. *Langmuir* 22:7732–7737. doi:10.1021/la0601399
- Balasubramaniam S, Kayandan S, Lin Y-N et al (2014) Toward design of magnetic nanoparticle clusters stabilized by biocompatible diblock copolymers for T₂-weighted MRI contrast. *Langmuir* 30:1580–1587. doi:10.1021/la403591z
- Barisik M, Atalay S, Beskok A, Qian S (2014) Size dependent surface charge properties of silica nanoparticles. *J Phys Chem C* 118:1836–1842. doi:10.1021/jp410536n
- Berret J-F, Schonbeck N, Gazeau F et al (2006) Controlled clustering of superparamagnetic nanoparticles using block copolymers: design of new contrast agents for magnetic resonance imaging. *J Am Chem Soc* 128:1755–1761. doi:10.1021/ja0562999
- Bin Na H, Song IC, Hyeon T (2009) Inorganic nanoparticles for MRI contrast agents. *Adv Mater* 21:2133–2148. doi:10.1002/adma.200802366
- Bulte JW, Kraitchman DL (2004) Iron oxide MR contrast agents for molecular and cellular imaging. *NMR Biomed* 17:484–499
- Caravan P, Ellison JJ, McMurry TJ, Lauffer RB (1999) Gadolinium(III) chelates as MRI contrast agents: structure, dynamics, and applications. *Chem Rev* 99:2293–2352
- Chen S, Andre P (2012) Colloidal syntheses of FePt nanoparticles. *Int J Nanotechnol* 9:39. doi:10.1504/IJNT.2012.044829
- Chen H, Yeh J, Wang L et al (2010a) Preparation and control of the formation of single core and clustered nanoparticles for biomedical applications using a versatile amphiphilic diblock copolymer. *Nano Res* 3:852–862. doi:10.1007/s12274-010-0056-y
- Chen S, Wang L, Duce SL et al (2010b) Engineered biocompatible nanoparticles for in vivo imaging applications. *J Am Chem Soc* 132:15022–15029. doi:10.1021/ja106543j
- Chou SW, Zhu CL, Neeleshwar S et al (2009) Controlled growth and magnetic property of FePt nanostructure: cuboctahedron, octapod, truncated cube, and cube. *Chem Mater* 21:4955–4961. doi:10.1021/cm902199p
- Chou SW, Shau YH, Wu PC et al (2010) In vitro and in vivo studies of FePt nanoparticles for dual modal CT/MRI molecular imaging. *J Am Chem Soc* 132:13270–13278. doi:10.1021/ja1035013
- Dai ZR, Sun S, Wang ZL (2001) Phase transformation, coalescence, and twinning of monodisperse FePt nanocrystals. *Nano Lett* 1:443–447. doi:10.1021/nl0100421
- Elsababy M, Wooley KL (2012) Design of polymeric nanoparticles for biomedical delivery applications. *Chem Soc Rev* 41:2545. doi:10.1039/c2cs15327k
- Green LA, Thuy TT, Mott DM et al (2014) Multicore magnetic FePt nanoparticles: controlled formation and properties. *RSC Adv* 4:1039. doi:10.1039/c3ra44319a
- Hirani B, Li J, Djurovich PI et al (2007) Cyclometallated iridium and platinum complexes with noninnocent ligands. *Inorg Chem* 46:3865–3875. doi:10.1021/ic061556b
- Huang G, Li H, Chen J et al (2014) Tunable T1 and T2 contrast abilities of manganese-engineered iron oxide nanoparticles

- through size control. *Nanoscale* 6:10404–10412. doi:[10.1039/c4nr02680b](https://doi.org/10.1039/c4nr02680b)
- Kim DK, Kan D, Veres T et al (2005) Monodispersed Fe-Pt nanoparticles for biomedical applications. *J Appl Phys* 97:50–52. doi:[10.1063/1.1860851](https://doi.org/10.1063/1.1860851)
- Kostevšek N, Žužek Rožman K, Arshad MS et al (2015) Multimodal hybrid FePt/SiO₂/Au nanoparticles for nanomedical applications: combining photothermal stimulation and manipulation with an external magnetic field. *J Phys Chem C* 119:16374–16382. doi:[10.1021/acs.jpcc.5b03725](https://doi.org/10.1021/acs.jpcc.5b03725)
- Lee DC, Mikulec FV, Pelaez JM et al (2006a) Synthesis and magnetic properties of silica-coated FePt nanocrystals. *J Phys Chem B* 110:11160–11166. doi:[10.1021/jp060974z](https://doi.org/10.1021/jp060974z)
- Lee J-H, Jun Y-W, Yeon S-I et al (2006b) Dual-mode nanoparticle probes for high-performance magnetic resonance and fluorescence imaging of neuroblastoma. *Angew Chem Int Ed Engl* 45:8160–8162. doi:[10.1002/anie.200603052](https://doi.org/10.1002/anie.200603052)
- Liang S, Zhou Q, Wang M et al (2015) Water-soluble L-cysteine-coated FePt nanoparticles as dual MRI/CT imaging contrast agent for glioma. *Int J Nanomedicine* 10:2325–2333. doi:[10.2147/IJN.S75174](https://doi.org/10.2147/IJN.S75174)
- Lu J, Liang M, Li Z et al (2010) Biocompatibility, biodistribution, and drug-delivery efficiency of mesoporous silica nanoparticles for cancer therapy in animals. *Small* 6:1794–1805. doi:[10.1002/sml.201000538](https://doi.org/10.1002/sml.201000538)
- Maenosono S, Saita S (2006) Theoretical assessment of FePt nanoparticles as heating elements for magnetic hyperthermia. *IEEE Trans Magn* 42:1638–1642. doi:[10.1109/TMAG.2006.872198](https://doi.org/10.1109/TMAG.2006.872198)
- Maenosono S, Suzuki T, Saita S (2008) Superparamagnetic FePt nanoparticles as excellent MRI contrast agents. *J Magn Magn Mater* 320:79–83. doi:[10.1016/j.jmmm.2008.01.026](https://doi.org/10.1016/j.jmmm.2008.01.026)
- Nandwana V, Nandwana V, Elkins KE et al (2007) Size and shape control of monodisperse FePt nanoparticles. *J Phys Chem C* 111:4185–4189. doi:[10.1021/jp068330e](https://doi.org/10.1021/jp068330e)
- Saita S, Maenosono S (2005) Formation mechanism of FePt nanoparticles synthesized via pyrolysis of Iron(III) ethoxide and platinum(II) acetylacetonate. *Chem Mater* 17:6624–6634. doi:[10.1021/cm051760h](https://doi.org/10.1021/cm051760h)
- Shevchenko EV, Talapin DV, Schnablegger H et al (2003) Study of nucleation and growth in the organometallic synthesis of magnetic alloy nanocrystals: the role of nucleation rate in size control of CoPt₃ nanocrystals. *J Am Chem Soc* 125:9090–9101. doi:[10.1021/ja029937l](https://doi.org/10.1021/ja029937l)
- Shin T, Choi Y, Kim S, Cheon J (2015) Recent advances in magnetic nanoparticle-based multi-modal imaging. *Chem Soc Rev* 44:4501–4516. doi:[10.1039/C4CS00345D](https://doi.org/10.1039/C4CS00345D)
- Slichter CP (1990) Principles of magnetic resonance. Springer, Berlin
- Stanford CJ, Dagenais M, Park J-H, DeShong P (2008) Real-time monitoring of siloxane monolayer film formation on silica using a fiber Bragg grating. *Curr Anal Chem* 4:356–361
- Sun S (2000) Monodisperse FePt nanoparticles and ferromagnetic FePt nanocrystal superlattices. *Science* 287:1989–1992. doi:[10.1126/science.287.5460.1989](https://doi.org/10.1126/science.287.5460.1989)
- Tanaka Y, Saita S, Maenosono S (2008) Influence of surface ligands on saturation magnetization of FePt nanoparticles. *Appl Phys Lett* 92:47–50. doi:[10.1063/1.2891083](https://doi.org/10.1063/1.2891083)
- Tanaka K, Narita A, Kitamura N et al (2010) Preparation for highly sensitive MRI contrast agents using core/shell type nanoparticles consisting of multiple SPIO cores with thin silica coating. *Langmuir* 26:11759–11762. doi:[10.1021/la1015077](https://doi.org/10.1021/la1015077)
- Taylor RM, Huber DL, Monson TC et al (2012) Structural and magnetic characterization of superparamagnetic iron platinum nanoparticle contrast agents for magnetic resonance imaging. *J Vac Sci Technol B Nanotechnol Microelectron* 30:2C101–2C1016
- Thanh NTK (2012) Magnetic nanoparticles: from fabrication to clinical applications. CRC Press, London
- Tong S, Hou S, Zheng Z et al (2010) Coating optimization of superparamagnetic iron oxide nanoparticles for high T₂ relaxivity. *Nano Lett* 10:4607–4613. doi:[10.1021/nl102623x](https://doi.org/10.1021/nl102623x)
- Verma A, Stellacci F (2010) Effect of surface properties on nanoparticle-cell interactions. *Small* 6:12–21
- Wang C, Hou Y, Kim J, Sun S (2007) A general strategy for synthesizing FePt nanowires and nanorods. *Angew Chem Int Ed* 46:6333–6335
- Wei H, Insin N, Lee J et al (2012) Compact zwitterion-coated iron oxide nanoparticles for biological applications. *Nano Lett* 12:22–25. doi:[10.1021/nl202721q](https://doi.org/10.1021/nl202721q)
- Wu XW, Liu C, Li L et al (2004) Nonmagnetic shell in surfactant-coated FePt nanoparticles. *J Appl Phys.* 95:6810–6812
- Xu C, Xu K, Gu H et al (2004) Dopamine as a robust anchor to immobilize functional molecules on the iron oxide shell of magnetic nanoparticles. *J Am Chem Soc* 126:9938–9939. doi:[10.1021/ja0464802](https://doi.org/10.1021/ja0464802)
- Yang H, Zhang J, Tian Q et al (2010) One-pot synthesis of amphiphilic superparamagnetic FePt nanoparticles and magnetic resonance imaging in vitro. *J Magn Magn Mater* 322:973–977. doi:[10.1016/j.jmmm.2009.11.039](https://doi.org/10.1016/j.jmmm.2009.11.039)
- Zeynali H, Sebt SA, Arabi H, Akbari H (2012) Size control of FePt nanoparticles produced by seed mediated growth process. *J Clust Sci* 23:1107–1117. doi:[10.1007/s10876-012-0506-7](https://doi.org/10.1007/s10876-012-0506-7)